

# Fracture Faces in the Cell Envelope of *Escherichia coli*

A. P. VAN GOOL AND N. NANNINGA

Laboratory of Electron Microscopy, University of Amsterdam, Amsterdam, The Netherlands

Received for publication 28 June 1971

Freeze-fracturing of *Escherichia coli* cells in the presence of 30% (v/v) glycerol resulted in a double cleavage of the cell envelope exposing two convex and two concave fracture faces ( $\overline{PM}$ ,  $\overline{PM}$  and  $\overline{CW2}$ ,  $\overline{CW2}$ ) with characteristic patterns. Complementary replicas revealed the relationship of the fracture faces to their corresponding fracture planes. The inner fracture plane splits the plasma membrane at one particular level. Apparently the outer fracture plane was located in the outer part of the wall, as it was separated by a layer ( $\overline{CW2}$ ) from the fractured profile ( $\overline{CW1}$ ) presumably corresponding to the murein layer. The outer fracture plane did alternate toward the cell periphery, exposing complementary smooth areas ( $\overline{CW3}$  and  $\overline{CW3}$ ). When cells were freeze-fractured in the absence of glycerol, the outer cell surface appeared as an etching face rather than a fracture face. A schematic representation of the relative location of the different fracture faces in the *E. coli* cell envelope is given.

Earlier electron microscopic studies have shown the complexity of the structure of *Escherichia coli* cell envelope. This information, derived from observation of intact cells or isolated cell envelopes, together with various chemical and enzymatic treatments, was discussed extensively by De Petris (5). More recently, freeze-fracturing has been used to study the ultrastructure of the cell wall and the plasma membrane of *E. coli* (1, 6, 11). The advantage of this technique is that it gives a three-dimensional image of the cell envelope. The different envelope layers observed in freeze-fractured cells were compared with the multilayered system observed in thin sections or shadowed preparations (5, 8-10, 15), and a model showing the spatial relationship of the different fracture faces was tentatively proposed (11). The present investigation attempted to define the relative position of the different fracture faces by using complementary freeze-fracture replicas.

## MATERIALS AND METHODS

**Culture and medium.** *E. coli* B was grown in Heart Infusion Broth (Difco Laboratories, Detroit, Mich.), at 37 C, with continuous shaking. Logarithmically growing cells were centrifuged at room temperature for 15 min at  $7,000 \times g$ . Glycerol at 30% (v/v) final concentration was added before harvesting. The pellet was mixed thoroughly with a few *Candida utilis* cells of a suitable size to facilitate finding the complementary

parts of fractured bacteria. *C. utilis* was grown at room temperature on malt agar slants.

**Freeze-fracturing.** The final suspension was inserted into four apposed specimen holders of the Denton DFE-3 freeze-fracture apparatus (Denton Vacuum Inc., Cherry Hill, N.J.). After freezing in Freon 22 (*E. I. duPont de Nemours & Co., Inc., Wilmington, Del.*), the specimens were transferred rapidly to a hinged mounting cap assembly in liquid nitrogen. The loaded cap assembly then was transferred to the precooled (about  $-180$  C) table of the freeze-fracture apparatus. The frozen specimens were fractured by tilting the specimen table. When the precooled fracture bar was held against the fracture arm of the specimen cap assembly, the upper part of the apposed specimen holders rotated  $180^\circ$ . After the specimens were etched for 3 min at  $-95$  C, they were replicated with platinum-carbon at a specimen temperature of  $-130$  to  $-140$  C. The replicas were floated on double-distilled water containing small amounts of detergent. They were cleaned in a solution of hypochlorite and washed twice in double-distilled water. The replicas then were picked up either on uncovered copper grids or on Formvar-coated grids reinforced with carbon, depending on the stability of the replica. In the absence of glycerol, some specimens were fractured in a Balzers apparatus as previously described (11).

**Electron microscopy.** Complementary replicas were scanned in a Philips EM200 or EM300 electron microscope operating at 80 kv. Corresponding areas on both replicas were identified by referring to the occurrence and morphology of the added yeast cells. Final electron micrographs were taken with the Philips EM300 electron microscope. In this report, micrographs are

printed in reverse, and direction of shadowing is indicated by an arrow in the lower right corner.

## RESULTS

In describing the results, we refer to the terminology previously used (11), taking into account the recent observations on membrane splitting in *Bacillus subtilis* (12).

Fracturing of *E. coli* cells frozen in the presence of 30% (v/v) glycerol commonly exposed four fracture faces in the cell envelope. Two of these fracture faces always appeared convex (Fig. 1). The inner convex fracture face of the plasma membrane ( $\overline{PM}$ ) was densely packed with particles; the outer convex fracture face ( $\overline{CW2}$ ) had a surface on which numerous small grooves and particles were irregularly distributed. The appearance of the inner convex fracture face ( $\overline{PM}$ ) did not vary with the presence or absence of glycerol. But the outer convex fracture face ( $\overline{CW2}$ ), only rarely observed in the absence of glycerol, was different: without glycerol, a relatively smooth fracture face was obtained (Fig. 2; see also reference 11, Fig. 4).

The prevalent concave fracture faces are shown in Fig. 3. On the inner concave face ( $\overline{PM}$ ), a sparse distribution of small particles and somewhat larger holes was present. The underlying concave face ( $\overline{CW2}$ ) had a very dense packing of flat particles with a diameter of approximately 10 nm (11). Irregularly shaped smooth areas ( $\overline{CW3}$ ) at a level lower than that of the closely packed elements were commonly observed (Fig. 4). Occasionally, an additional profile ( $\overline{CW1}$ ) could be seen between the concave fracture faces  $\overline{PM}$  and  $\overline{CW2}$  (Fig. 3). However, no information about the structure of this area was obtained as only its profile was revealed (11).

Complementary replicas were made to compare the different fracture faces. Corresponding fracture faces are shown in Fig. 5 and 6. The outer convex fracture face ( $\overline{CW2}$ ) described in Fig. 1 is apposed to the fracture face composed of densely packed elements ( $\overline{CW2}$ ) shown in Fig. 3. It should be noted that the surroundings of the exposed cell envelope faces (Fig. 5) are not complementary to each other. This might result from slightly different etching conditions in the two specimens. In Fig. 6, the corresponding outer fracture faces ( $\overline{CW2}$  and  $\overline{CW2}$ ) are visible together with the convex and concave fracture faces ( $\overline{PM}$  and  $\overline{PM}$ ) of the plasma membrane. The intermediate fracture profile ( $\overline{CW1}$ ) is apparent on both replicas. This profile disappears toward the outer surface at the left pole of the upper cell, exposing a rough-textured gap between the fractured profiles of  $\overline{PM}$  and  $\overline{CW2}$ .

The smooth areas ( $\overline{CW3}$ ), shown in Fig. 4, also appeared on complementary replicas, lo-

cated at the same sites on both fracture faces. Because the convex fracture face ( $\overline{CW2}$ ) appeared rather irregular and rough, these smooth areas on the corresponding concave face ( $\overline{CW2}$ ) could be observed more clearly. Interruptions in the close arrangement of flat particles ( $\overline{CW2}$ ) occurred freely at the boundary of the cell (Fig. 4, arrow 1). Thus, no structural difference between the smooth areas ( $\overline{CW3}$ ) and the medium surrounding the cell was observed. However, such an area appeared also at a different level, indicated by a ridge at the cell boundary (Fig. 4, arrow 2). The complementary part of a smooth area extending towards the periphery of the cell is shown in Fig. 7. We have no satisfactory explanation for the appearance of the smooth areas at two different levels.

When *E. coli* cells were harvested in early exponential growth and treated with lysozyme in a stabilizing medium (2), spheroplasts were formed after a 1:1 dilution of the stabilizing agent with 10 mM tris(hydroxymethyl)amino-methane buffer (pH 8.0). Freeze-fracturing of spheroplasts in 0.25 M sucrose revealed typical fracture faces of the plasma membrane. The remaining cell wall detached from the plasma membrane was observed in cross-fracture only.

## DISCUSSION

Multiple fracturing of the frozen cell envelope of *E. coli* was described in earlier reports (6, 11), and a three-dimensional reconstruction has been given (11). The introduction of the technique of complementary freeze-fracture replicas by Steere and Moseley (Proc. 27th Annu. Meet. Electron Microsc. Soc. Amer., p. 202-203) facilitated the visualization of the spatial relationship of convex and concave faces. In the present investigation, this method was used to refine the previous model (11), which was based on single replicas. The best results were obtained, especially with respect to the outer fracture plane, when cells were frozen in 30% (v/v) glycerol. Under these conditions, freeze-fracturing commonly exposed four faces in the cell envelope (Fig. 1, 3). Complementary replicas revealed directly their relationship to an inner and to an outer fracture plane (Fig. 5, 6). The outer surface of the cell ( $\overline{CW4}$ ), indicated by the appearance of flagella (Fig. 2), was not observed unless the fractured cells were etched in the absence of glycerol.

The inner fracture plane revealed the convex face ( $\overline{PM}$ ) densely covered with particles; the corresponding concave face ( $\overline{PM}$ ) had fewer particles and small holes (Fig. 6), which appeared less frequently at lower glycerol concentrations. It has been shown earlier, on the basis of slightly plasmolyzed cells, that these faces belong to the

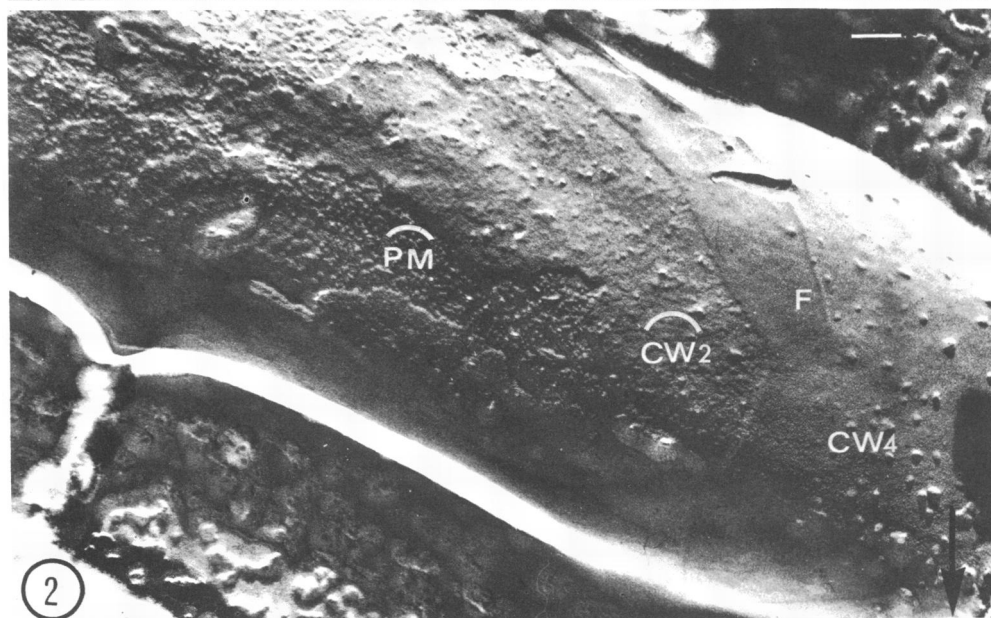
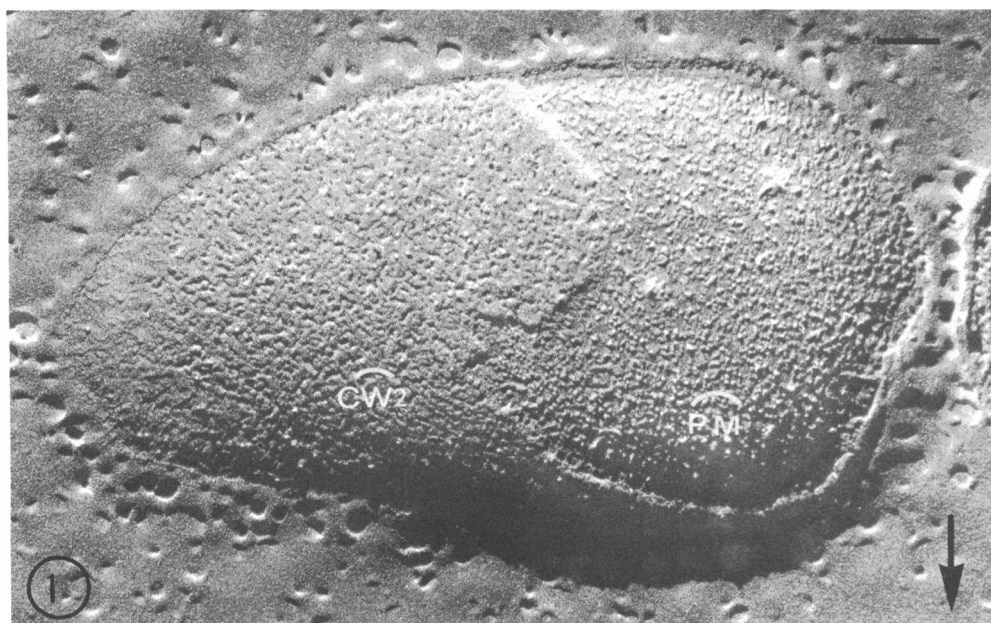


FIG. 1. Convex fracture faces of *Escherichia coli* cell envelope in the presence of 30% (v/v) glycerol.  $\widehat{PM}$ , convex fracture face of plasma membrane;  $\widehat{CW2}$ , convex fracture face of cell wall. Bar in upper right corner, Fig. 1-8, equals 0.1  $\mu\text{m}$ .

FIG. 2. Convex fracture faces in the absence of glycerol.  $\widehat{PM}$ , convex fracture face of plasma membrane;  $\widehat{CW2}$ , convex fracture face of cell wall;  $\widehat{CW4}$ , outer cell wall surface exposed by etching; F, flagellum.

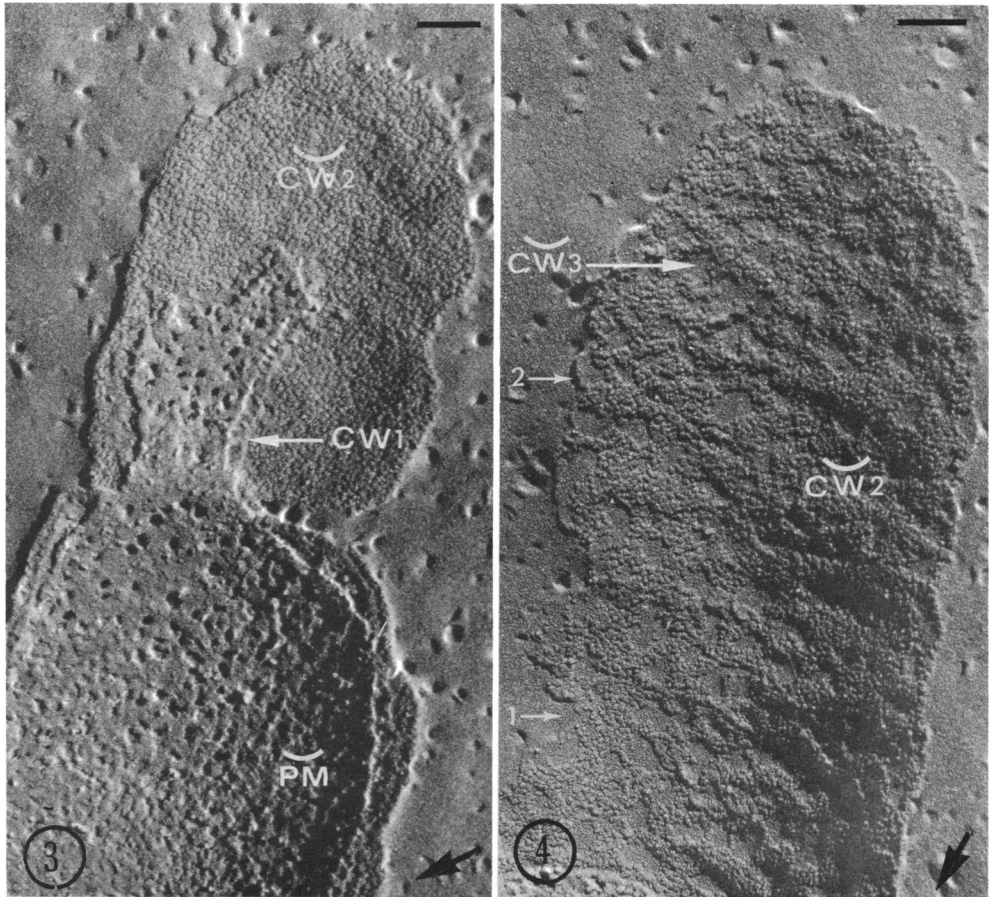


FIG. 3. Concave fracture faces.  $\overline{PM}$ , concave fracture face of plasma membrane;  $\overline{CW1}$  and  $\overline{CW2}$ , concave fracture faces of cell wall.

FIG. 4. Smooth areas ( $\overline{CW3}$ ) interrupting the  $\overline{CW2}$  fracture face. Arrow 1, smooth area continuous with surroundings of cell; arrow 2, smooth area at a level higher than surroundings of the cell.

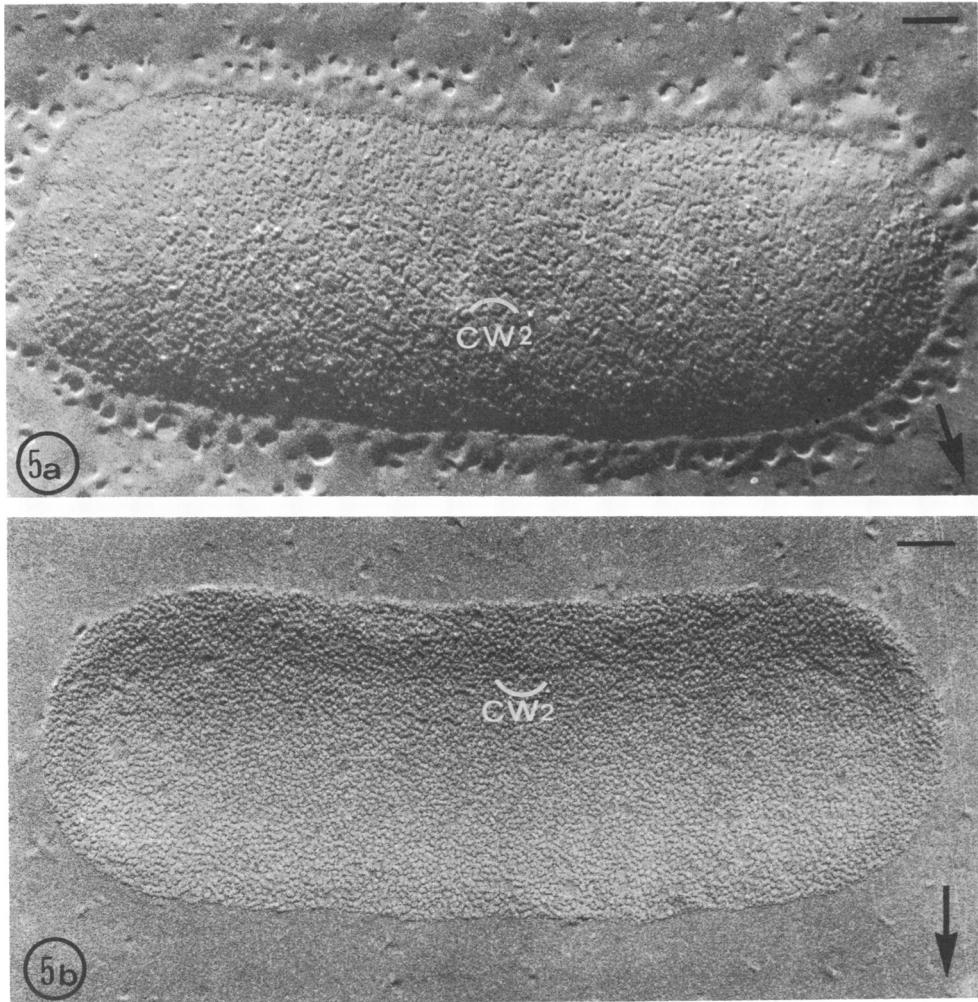


FIG. 5. Complementary fracture faces in cell wall. a,  $\widehat{CW}_2$ , convex fracture face; b,  $\check{CW}_2$ , concave fracture face.

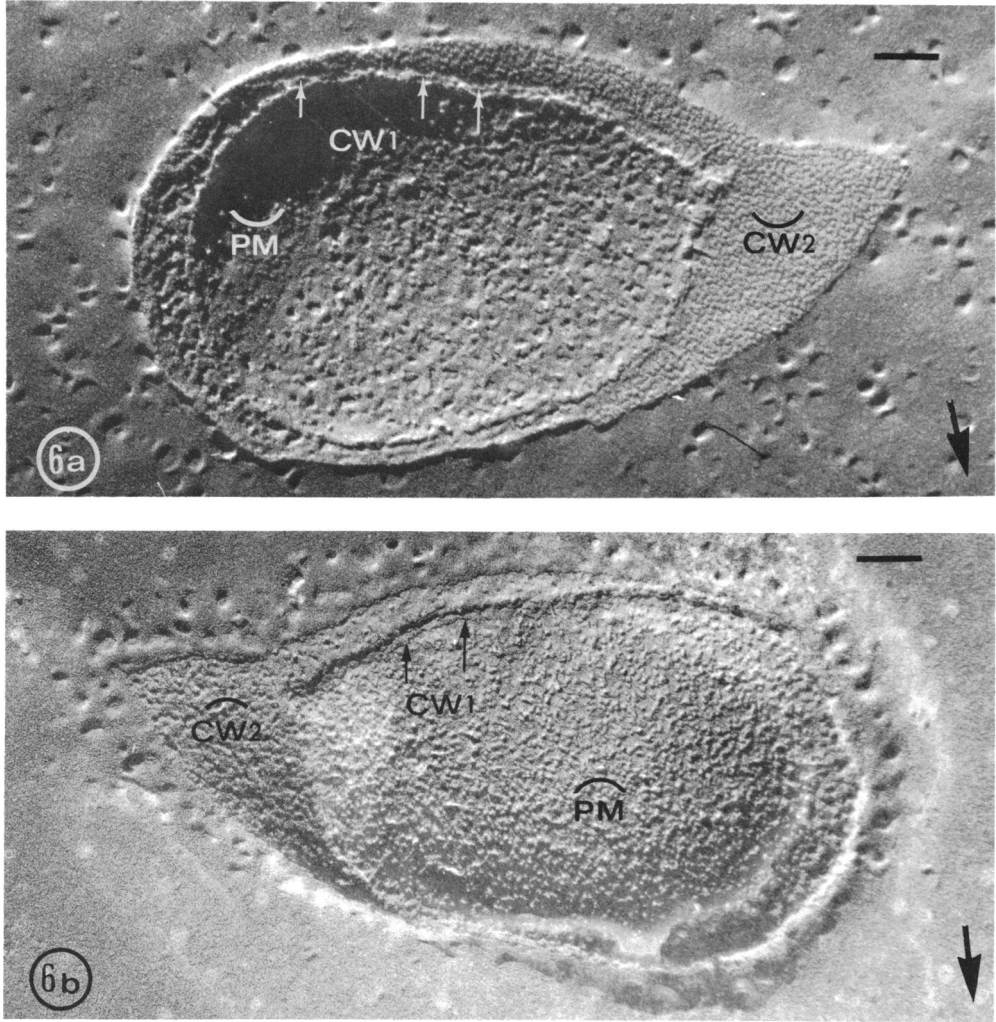


FIG. 6. Complementary fracture faces in cell envelope.  $\widehat{PM}$  and  $\overline{PM}$ , fracture faces of plasma membrane;  $\widehat{CW2}$  and  $\overline{CW2}$ , fracture faces of cell wall;  $CW1$ , fracture profile between PM and CW2.

plasma membrane (6, 11). The same fracture faces have been observed in spheroplasts (*unpublished data*). Thus, the presence of a unique fracture plane exposing, in intact cells as well as in spheroplasts, fracture faces from which no appreciable amount of water disappears upon etching may be considered an argument for the splitting of the plasma membrane along inner hydrophobic regions as discussed extensively by Branton (3). A unique fracture plane also was inferred by Sleytr (14) by studying complementary fracture faces in protoplasts of *B. stearothermophilus*. From observations on complementary replicas and thin sections of freeze-fractured cells, more direct evidence has been given for the splitting of the plasma membrane in *B. subtilis* (12). Therefore, the concept of membrane splitting, as contrasted to cleavage along both surfaces, may be a general feature of the freeze-fractured bacterial plasma membrane.

In some instances, the convex fracture face showed a netlike arrangement of particles (Fig. 8; reference 6). This pattern was revealed on the complementary fracture face only with respect to the areas devoid of particles.

The outer fracture plane revealed a rough convex face ( $\overline{CW2}$ ), with the complementary concave face characterized by the dense arrangement of flat elements (6, 11) about 10 nm in diameter (Fig. 5, 6). Originally, these elements were interpreted as corresponding to globular lipoprotein covalently bound to the murein (11). This seemed plausible, as Braun and Sieglin recently proposed a periodicity of 10.3 nm for the attachment sites of lipoprotein molecules to the murein layer (4; *see also* reference 7). However, Fig. 6 shows that the outer fracture plane is separated from CW1 by the convex complement

( $\overline{CW2}$ ) of the concave layer of closely packed elements ( $\overline{CW2}$ ). The outer fracture plane also has interruptions near the cell periphery in the  $\overline{CW2}$  fracture face, exposing smooth areas (Fig. 4,  $\overline{CW3}$ ). These smooth areas also were observed on the complementary fracture face ( $\overline{CW2}$ ), and appeared at different levels with respect to the medium surrounding the cell (Fig. 4, arrows 1 and 2; Fig. 7). Therefore, we tend to conclude that the outer fracture plane is located in the outer part of the cell wall. Using spheroplasts would allow a more precise localization. But unfortunately no fracture plane was observed in the detached cell wall. Schnaitman recently found substantial amounts of phospholipid and protein in isolated *E. coli* cell wall fragments

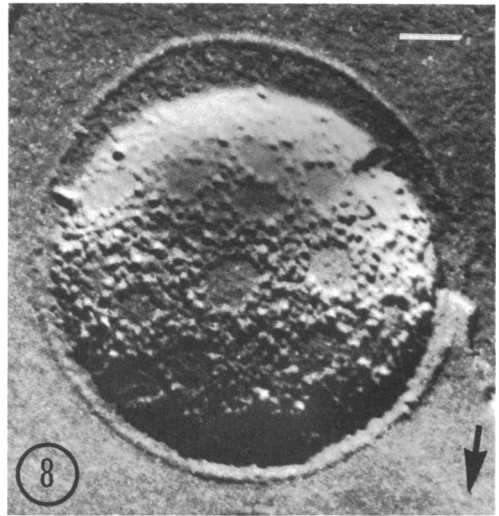


FIG. 8. Convex fracture face of plasma membrane with netlike arrangement of particles.

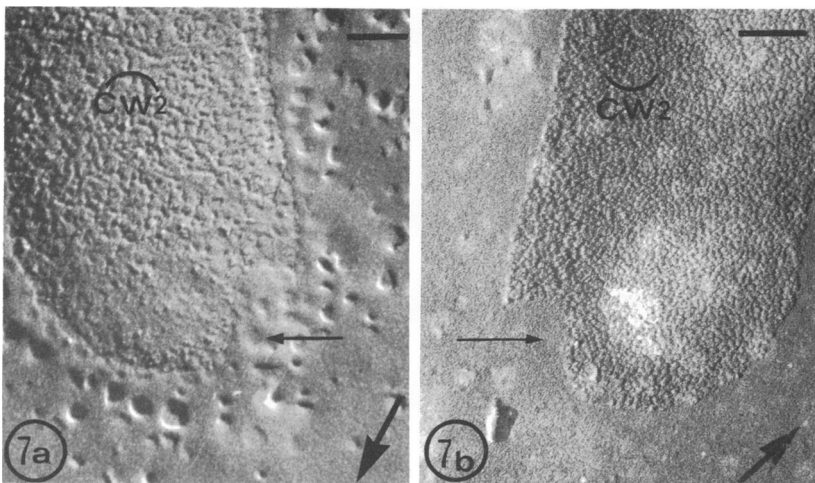


FIG. 7. Complementary replicas of a smooth area (arrows) extending freely into surrounding medium.

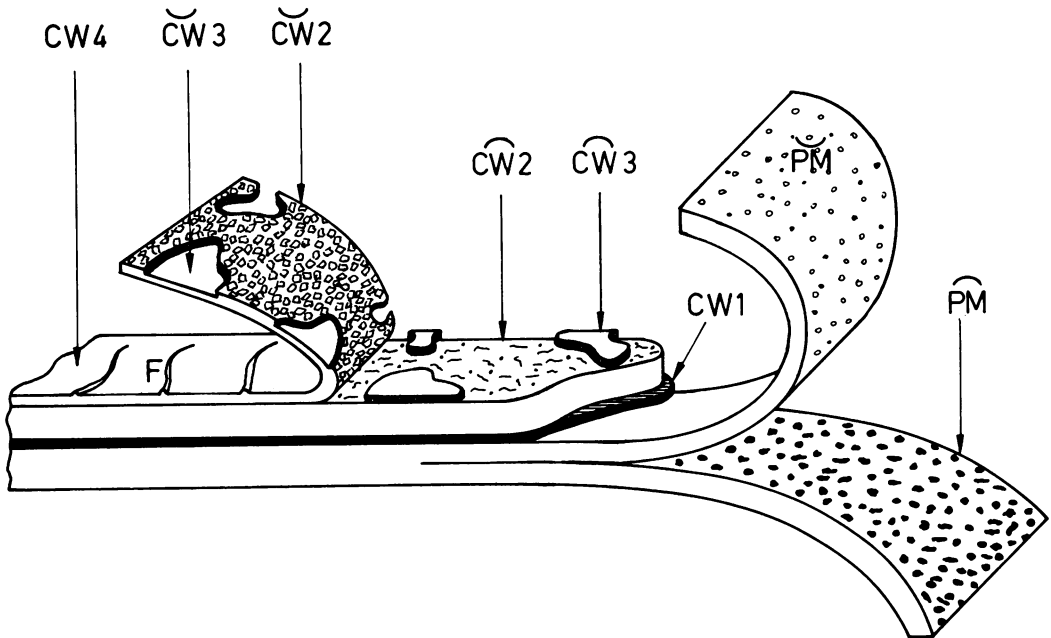


FIG. 9. Reconstruction of freeze-fractured *Escherichia coli* cell envelope indicating relative positions of fracture faces. (Fracture face dimensions are arbitrary.)  $\overline{PM}$  and  $\overline{PM}$ , fracture faces in plasma membrane;  $\overline{CW1}$ , presumed fracture profile of murein layer;  $\overline{CW2}$ ,  $\overline{CW2}$  and  $\overline{CW3}$ ,  $\overline{CW3}$ , fracture faces in cell wall;  $\overline{CW4}$ , outer surface of wall revealed by etching; *F*, flagella. The outer surface of the plasma membrane shown here was never observed.

(13). About 70% of the protein was identified as a single species (molecular weight 44,000) which was not bound to the murein layer. Schnaitman assumed that this protein is located in the outer cell wall, forming a lipoprotein membrane with the phospholipid in which lipopolysaccharide is inserted. This evidence suggests that the outer fracture plane results from the splitting of the outer membrane, possibly exposing the single protein species as the concave fracture face ( $\overline{CW2}$ ).

A schematic representation of the various fracture faces in the cell envelope is given in Fig. 9. Of course, the technique of freeze-fracturing does not give direct information on the chemical constitution of the exposed structures.

#### ACKNOWLEDGMENTS

We thank D. C. Barker for reading the manuscript and Frida C. Tijssen for technical assistance. A.P.V.G. was supported by the Belgisch National Fonds voor Wetenschappelijk Onderzoek. We appreciate the help of W. Moll in preparing Fig. 9.

#### LITERATURE CITED

- Bayer, M. E., and C. C. Remsen. 1970. Structure of *Escherichia coli* after freeze-etching. *J. Bacteriol.* **101**:304-313.
- Birdsell, D. C., and E. H. Cota-Robles. 1967. Production and ultrastructure of lysozyme and ethylenediamine-tetraacetate-lysozyme spheroplasts of *Escherichia coli*. *J. Bacteriol.* **93**:427-437.
- Branton, D. 1969. Membrane structure. *Annu. Rev. Plant Physiol.* **20**:209-238.
- Braun, V., and U. Sieglin. 1970. The covalent murein-lipoprotein structure of the *Escherichia coli* cell wall. The attachment site of the lipoprotein on the murein. *Eur. J. Biochem.* **13**:336-346.
- De Petris, S. 1967. Ultrastructure of the cell wall of *Escherichia coli* and chemical nature of its constituent layers. *J. Ultrastruct. Res.* **19**:45-83.
- Fiil, A., and D. Branton. 1969. Changes in the plasma membrane of *Escherichia coli* during magnesium starvation. *J. Bacteriol.* **98**:1320-1327.
- Fischman, D. A., and G. Weinbaum. 1967. Hexagonal pattern in cell walls of *Escherichia coli* B. *Science* **155**:472-474.
- Hofschneider, P. H., and H. H. Martin. 1968. Diversity of surface layers in L-forms of *Proteus mirabilis*. *J. Gen. Microbiol.* **51**:23-33.
- Martin, H. H., and H. Frank. 1962. Quantitative Bausteinanalyse der Stützmembran in der Zellwand von *Escherichia coli* B. *Z. Naturforsch.* **17B**:190-196.
- Murray, R. G. E., P. Steed, and H. E. Elson. 1965. The location of the mucopeptide in sections of the cell wall of *Escherichia coli* and other gram-negative bacteria. *Can. J. Microbiol.* **11**:547-560.
- Nanninga, N. 1970. Ultrastructure of the cell envelope of *Escherichia coli* B after freeze-etching. *J. Bacteriol.* **101**:297-303.
- Nanninga, N. 1971. Uniqueness and location of the fracture plane in the plasma membrane of *Bacillus subtilis*. *J. Cell Biol.* **49**:564-570.
- Schnaitman, C. A. 1970. Protein composition of the cell wall and cytoplasmic membrane of *Escherichia coli*. *J. Bacteriol.* **104**:890-901.
- Sleytr, U. 1970. Fracture faces in cells and protoplasts of *Bacillus stearothermophilus*. *Protoplasma* **71**:295-312.
- Weidel, W., H. Frank, and H. H. Martin. 1960. The rigid layer of the cell wall of *Escherichia coli* strain B. *J. Gen. Microbiol.* **22**:158-166.